Solid-state effects on Rayleigh-scattering experiments: Limits for the free-atom approximation

O. D. Gonçalves
Instituto de Física da Universidade Federal do Paraná, Caixa Postal 68528, Rio de Janeiro, 21941, Brazil

C. Cusatis and I. Mazzaro
Departamento de Física da Universidade Federal do Paraná, Caixa Postal 19091, Curitiba, 81531, Brazil
(Received 16 September 1992)

Elastic scattering of photons from solid samples of Pb, Pt, and W was measured in order to investigate the limits within which scattering experiments can be described as being due to free atoms. The experiments were performed with photons of 22.1 keV from an x-ray tube and from an ^{241}Am (59.54 keV) γ source, providing a momentum transfer ranging from $x=0.1$ to 2.0 Å^{-1}. It is shown that the low-momentum-transfer limit for the free-atom approximation will depend on the scatterer, temperature, geometrical resolution, and on the accuracy of the experiment.

PACS number(s): 32.80.Cy, 78.70.Ck

INTRODUCTION

Measurements of elastic scattering of photons by bound atomic electrons, known as Rayleigh scattering, are an important test of methods to calculate scattering amplitudes. They are also important in measuring higher-order scattering amplitudes such as Delbruck scattering in which the amplitude of the effect corresponds to a few percent of the Rayleigh-scattering amplitude [1]. In the low-energy range, near absorption edges, an accurate knowledge of the elastic scattering cross section is particularly important [2].

Up to now, several experiments with photon energies ranging from keV to MeV have been performed, most of them with metals as scatterers. A review is presented in Refs. [3,4]. The extent to which theories agree with the experimental data is still not completely clear, but the most successful theoretical approach is clearly the second-order perturbation theory, as developed by Kissel and Pratt [3,4], mainly for energies above 100 keV with a corresponding momentum transfer $x>2$ Å^{-1}, where $x=(E/12.4)\sin(\theta/2)$, E is in keV, and θ is the scattering angle.

There are very few data on Rayleigh scattering below $x=2$ Å^{-1}. Those data are not conclusive, and some of them, when compared to theory, show discrepancies up to 30% [5]. An explanation of this discrepancy is not given, even if the possibility of interference between photons scattered by different atoms is mentioned. Bragg scattering is probably responsible for the discrepancies pointed out in [5].

To our knowledge, the only systematic measurement showing the transition between the environment scattering and the free-atom scattering regimes is one of our former work [6]. There, we have reported the occurrence of diffraction peaks due to Bragg scattering in photon scattering differential cross sections for polycrystalline samples.

The aims of the present work are as follows: (1) To show how the transition between Bragg and Rayleigh scattering can be understood by means of simple theoretical considerations. In other words, since all solid samples have a periodic structure, we want to show why it is possible to consider a solid sample as being composed of free atoms, and to show in which region of momentum transfer this approximation is expected to be valid.

(2) To determine the minimum momentum-transfer limit by comparison between measurements of elastic scattering using solid samples with theoretical results using the free-atom approximation. Two sets of experiments were performed with different photon energies and geometrical resolutions. The use of different energies and geometrical resolution provides quantitative information about how these parameters affect the detection of diffraction peaks in elastic scattering.

THEORY

Elastic scattering amplitudes of photons by atoms, with photon energy ranging from a few keV to MeV, are usually calculated with the assumption that the atoms are free. The most common of such calculations are based on the form-factor approximation either in the nonrelativistic, relativistic, or in the modified relativistic version. Extensive tables were published by Schaupp *et al.* [7] and Hubbel and co-workers [8,9]. In this approximation, the scattering intensity is taken as the scattering intensity due to a free electron multiplied by the Fourier transform of the electronic density. Different ways of obtaining the electron wave functions correspond to different form factors. The best agreement with experimental data was obtained with the modified relativistic form factor, also called the G factor. The wave functions are in this case obtained from a Dirac-Hartree-Fock calculation considering spherical symmetry for the atom.

The most complete (and computer-time-consuming) approach is the second-order perturbation theory, first developed by Brown *et al.* [10] and improved by Kissel and Pratt [3,4]. The method is still a one-particle model, but considers all possible (permitted and forbidden) transitions to intermediate states in the scattering process.

Both methods are described in detail in Ref. [3]. A comparison between different theories and experimental data for $x > 1$ can be found in Refs. [11] and [3].

For x less than 2 Å^{-1}, the cooperative effects due to the aggregate state of the atoms in the sample may render meaningless the direct comparison of experimental data on Rayleigh cross sections with results of free-atom theories. Even the lack of periodicity in the atomic arrangement of amorphous solids, liquids, or nonmonoatomic gas does not avoid the conditioning of the elastic scattering due to the finite size of the molecules. For very low x values, accurate elastic scattering measurements made with x-rays have been reported by different authors [12–15] in studies of condensed-matter structure. Most of those measurements were performed just by detecting the diffraction peaks.

In that area it is usual to suppose that the elastic scattering of photons by atomic electrons is well described by the form-factor approximation. Although not completely true, this will be assumed here in order to show how the transition between the structure and the free-atom scattering regimes can be understood.

Following Warren [16], for small momentum transfer (where the form-factor approximation is expected to be valid), the intensity of elastic scattered radiation (energy per unit area per unit time at a distance R of the scatterer) from noncrystalline or polycrystalline samples with randomly oriented grains is given in electron units by,

$$I_s = I_e \sum_m \sum_n f_m f_n e^{i\mathbf{K}\cdot(\mathbf{R}_m - \mathbf{R}_n)} ,$$
$$I_e = r_0^2/R^2[(1+\cos^2\theta)/2] , \tag{1}$$

where I_e is the Thomson scattering intensity at a distance R from the electron, I_0 is the intensity of incident radiation, r_0 is the classical electron radius, θ is the scattering angle, f_m, f_n are the atomic form factors, $\mathbf{R}_m$ ($\mathbf{R}_n$) is the position of the mth (nth) atom in the cell, and $\mathbf{K}$ is the momentum transfer, $|\mathbf{K}| = 4\pi x$.

Thermal vibration causes small displacements of the m atom from $\mathbf{R}_m$ to $\mathbf{R}_m + \boldsymbol{\mu}_m$ where $\boldsymbol{\mu}_m$ is the instantaneous displacement of the mth atom. For polycrystalline samples with cubic unit cell and one atom per cell (monoatomic), the intensity becomes

$$I_s = I_e f^2 \sum_m \sum_n e^{i\mathbf{K}\cdot(\mathbf{R}_m - \mathbf{R}_n)} e^{i\mathbf{K}\cdot(\boldsymbol{\mu}_m - \boldsymbol{\mu}_n)} . \tag{2}$$

The $e^{i\mathbf{K}\cdot(\boldsymbol{\mu}_m - \boldsymbol{\mu}_n)}$ term is the only time-dependent term in Eq. (2). Since measurements are carried over a long period of time compared with temperature-induced oscillations, this term must be taken as a time average.

With the oversimplified hypothesis of independent vibration of the atoms, Debye theory [16] predicts the scattered intensity to be

$$I_s = I_e f^2 N(1-e^{-2M}) + I_e f^2 e^{-2M} \sum_m \sum_n e^{2\mathbf{K}\cdot(\mathbf{R}_m - \mathbf{R}_n)} , \tag{3}$$

where

$$2M = 2B(K/4\pi)^2 = 2Bx^2 , \tag{4}$$

e^{-2M} is the Debye factor, and B the temperature factor.

The first term in Eq. (3) is the thermal diffuse scattering (TDS) intensity in the independent-atomic-vibration model. This term tends to $I_e N f^2$ for large values of x, i.e., to the free-atom-scattering intensity.

Even considering the more complete theory of coupled atomic vibrations (phonons), the TDS intensity for large x tends to the free-atom-scattering intensity. This theory predicts that the TDS intensity scattered by a polycrystalline sample [with a cubic-face-centered (fcc) unit cell, for example], does not increase monotonically with the momentum transfer but has maxima coincident with the reciprocal-lattice points. The widths of such peaks are larger than the corresponding Bragg ones. Between the reciprocal lattice points, the results of the phonon scattering theory tends to the Debye-theory results, i.e., the scattering increases with x and with the atomic vibration amplitude.

The second term in Eq. (3) is responsible for the ordinary crystalline diffraction and decreases with growing x due to the form factor and due to e^{-2M}. For small vibration amplitudes, the e^{-2M} factor can become small enough for the diffraction to be important. This can be true even for relatively large momentum transfer (but still in the context of the diffraction formalism).

Table I shows the B values for W, Pt, and Pb obtained from Ref. [17]. It is possible to see the dependence of the scattered intensities on the sample and on the temperature. The last three columns show the x value for which $100e^{-2M}$ will be 0.1%, 1.0%, and 5.0% respectively. The diffracted intensity will be reduced by TDS to 1% of the corresponding intensity without considering the effect for W (the smallest B), for $x = 3.4$ Å^{-1} at $T = 293$ K and for $x = 6.8$ Å^{-1} at $T = 0$ K. For lead, the same condition will be reached for much smaller values of x: $x = 0.96$ Å^{-1} at $T = 293$ K and $x = 3.7$ Å^{-1} at $T = 0$ K.

The angular resolution of the experiment will also be important. At higher energies the distance between the reciprocal-lattice points will be smaller, which means more Bragg peaks in the acceptance angle. Moreover, the net peak area will be smaller than the area under the peak (that is, the TDS scattering intensity). If the angular resolution of the scattering measurement is poor, the diffraction peaks will not be detected. The aimed accura-

TABLE I. Theoretical x values for which Bragg diffraction intensities are reduced to 0.1%, 1.0% and 5.0% of the intensity diffracted by a crystalline lattice without vibrations, for temperatures 0 and 273 K. Values of B are an average of the values published by International Tables for X-ray Crystallography [17].

Temperature (K)	Element	Debye thermal parameter B	x value (Å^{-1}) 0.1%	1.0%	5.0%
0	Pb	0.17	4.5	3.7	3.0
0	Pt	0.06	7.6	6.2	5.0
0	W	0.05	8.3	6.8	5.5
293	Pb	2.5	1.2	0.96	0.80
293	Pt	0.25	3.7	3.0	2.4
293	W	0.20	4.2	3.4	2.7

cy of the results will determine the necessary minimum angular resolution.

With the above considerations we have shown that the application of the free-atom approximation will depend on the sample (chemical element and atomic structure) and on experimental parameters (momentum transfer, geometrical resolution of the setup, and temperature). The next section presents experimental data obtained in order to investigate these limits (unless the temperature factor) for polycrystalline samples.

EXPERIMENTAL PROCEDURE

59.54-keV experiments

The measurements with photons of 59.54 keV were performed at the Instituto de Física of the Universidade Federal do Rio de Janeiro. Laminated foils of W, Pt, and Pb with thicknesses of 200, 120, and 150 μm, respectively, were used as scatterers. The photon source was a 200-mCi ^{241}Am γ source from Amershan. Source and scatterer were placed in a vacuum tube to eliminate scattering in the air. The detection system was a Ge-Li detector, conventional spectroscopic electronic, and a multichannel analyzer. Details of the apparatus are reported elsewhere [6].

The results are presented in number of scattered photons per unit time (N_{scatt}), corrected for attenuation N_{corr}. The relation with the cross section is given by

$$N_{\text{corr}} = N_{\text{scatt}} \frac{1}{F_{\text{att}}} = N_0 N_{\text{at}} \frac{d\sigma}{d\Omega} ,$$

where $1/F_{\text{att}}$ is the attenuation correction factor, $d\sigma/d\Omega$ is the differential cross section in cm^2, N_0 is the number of incident photons per unit time, and N_{at} is the number of illuminated atoms per cm^2. For normal incidence (angle between incidence direction and sample surface $\theta_i = 90°$),

$$\frac{1}{F_{\text{att}}} = \frac{(e^{-\mu a} - e^{-\mu a/\cos\theta})}{a\mu(1-1/\cos\theta)} ,$$

where μ is the total attenuation coefficient in cm^2/g, a is the scatterer thickness in g/cm^2, and θ is the scattering angle. The angular resolution was 0.3° for $\theta < 20°$ and 0.5° for $\theta > 20°$ resulting in a momentum-transfer resolution Δx of about 0.02 Å^{-1}.

22.1-keV experiment

The measurements with 22.1-keV photons were performed at the Departmento de Física of the Universidade Federal do Parana, using the characteristic Ag $K\alpha$ lines

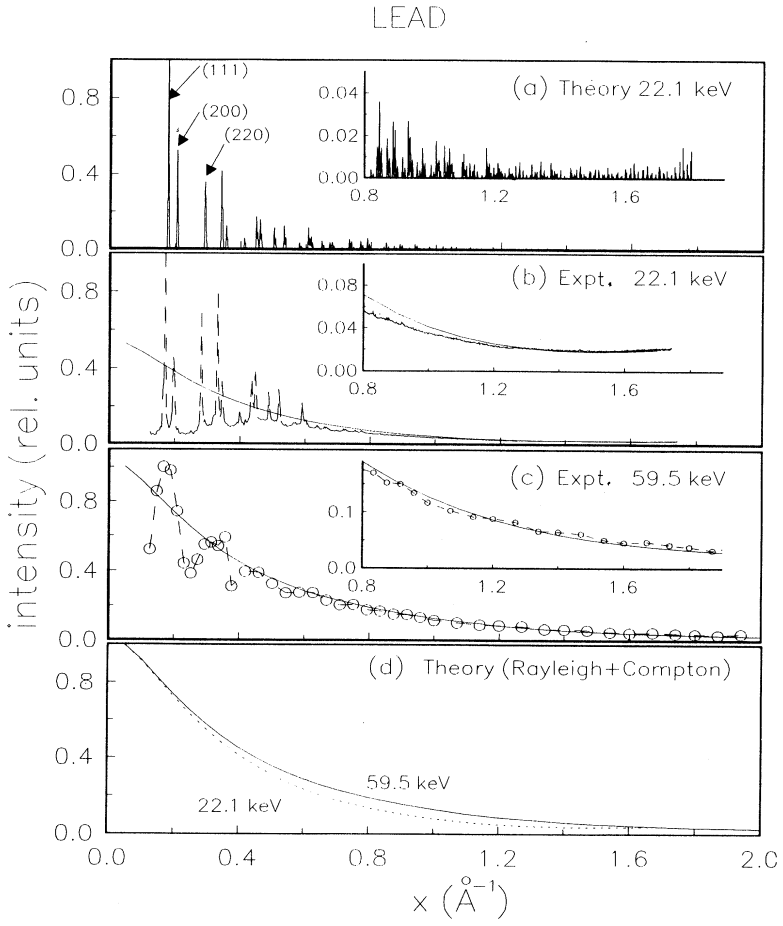

FIG. 1. Results for Pb. (a) Theoretical Bragg scattering intensities corrected for TDS. (b) Scattering intensities for 22.1-keV photons: dashed lines, experimental data; solid line, theoretical data for the free atom including Compton scattering. (c) Differential scattering cross sections for 59.56-keV photons: dashed line, experimental data; solid line, theoretical data for the free atom including Compton scattering. Experimental errors in the intensity ($<5\%$) and in the momentum transfer ($\delta x = 0.02$ Å^{-1}) are smaller than the point size. (d) Theoretical differential cross section ($d\sigma/d\omega$) for the free-atom case. The small figures are just part of (a), (b), and (c) with another scale.

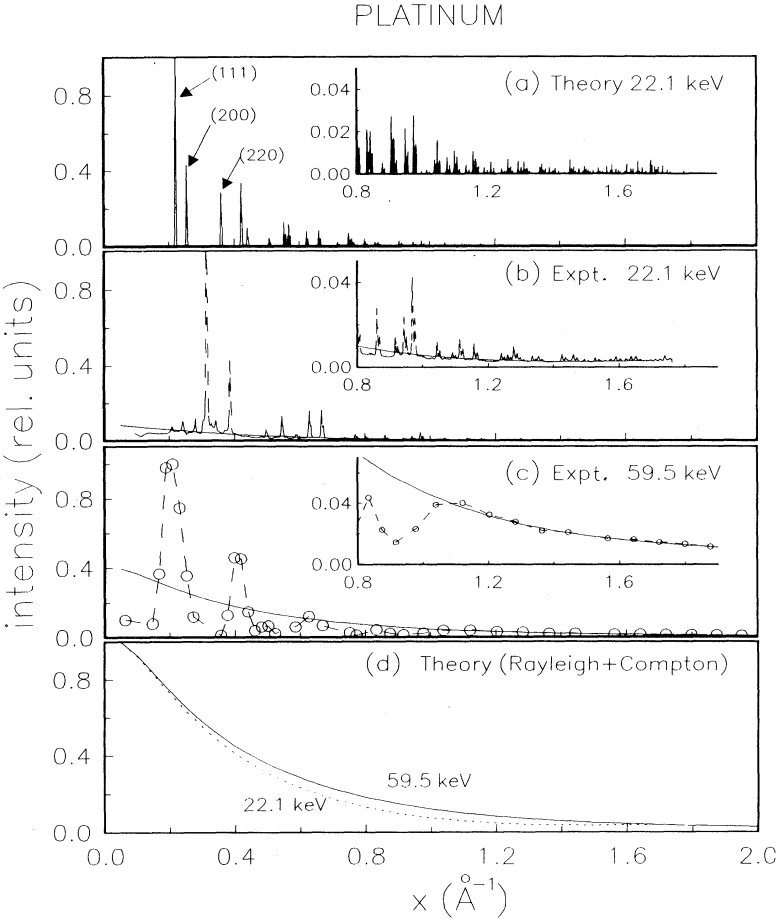

FIG. 2. Same as Fig. 1 for Pt. Some peaks modified by preferential grain orientation are pointed out by arrows.

from an x-ray tube in the conventional Bragg-Bretano focusing powder diffractometer with divergent and scattering slits equal to 2° and receiving slits of 0.3 mm. The same scatterers from the γ experiment were measured using a scintillation NaI detector with a single-channel analyzer. For some scattering angles, the photon-energy spectrum was measured with a Ge HP detector in order to compare the measured elastic area with the corresponding one obtained with the NaI detector.

The lower-energy resolution of the NaI did not worsen the resulting data error because, for this energy, the Compton intensity is not comparable with the elastic intensity, being of about 1% for the worst case (W, $x=2.0$ Å^{-1}). It was not necessary to correct the measured number of scattered photons for absorption since at this energy and angular range the sample thickness can be supposed to be infinite ($e^{-\mu t}=10^{-7}$), which implies the same correction factor for all measured angles.

The angular resolution of the system was 0.1°, resulting in a momentum-transfer resolution of 0.002 Å^{-1}. It should be noted that in spite of the poorer resolution $\Delta E/E$ of the x-ray line (10^{-4}) when compared with the γ line (10^{-6}), the resulting momentum-transfer resolution in the x-ray case is 10 times better.

RESULTS AND CONCLUSIONS

Experimental results with theoretical predictions are shown in Figs. 1–3, all of them normalized to 1. The curves labeled (a) are the result of calculations of diffraction intensities considering reduction of the diffraction peaks due to TDS. The resulting TDS intensities (which would increase the intensity between the Bragg peaks) were not included. The data were obtained by using the second term of Eq. (3) and data from Ref. [17].

The curves labeled (b) are the experimental results obtained with photons of 22.1 keV, and those labeled (c) are experimental results of the 59.54-keV experiment. The medium-dashed in (b) and (c) lines are just a guide to the eye. The solid lines are theoretical results obtained for the free-atom case with the modified form-factor theory [7] corrected to include Compton scattering. The Compton scattering intensities were obtained by using the incoherent-scattering-factor approximation [8]. Since the data are not absolute measurements, the theoretical curves are normalized to fit the experimental data in the high-x region.

The theoretical results for both energies are plotted in Figs. 1(d), 2(d), and 3(d), normalized to 1 to compare both

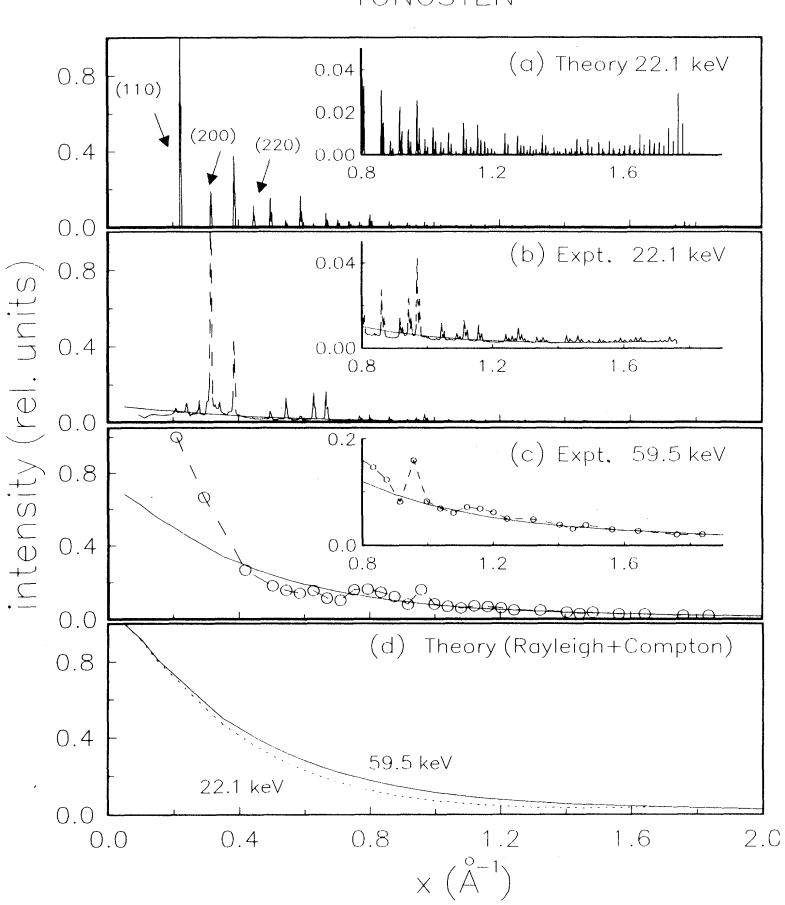

FIG. 3. Same as Fig. 1 for W. Some of the small peaks in (b) that do not appear in (a) are due to the unfiltered Ag $K\beta$ radiation. Some peaks modified by preferential grain orientation are pointed with arrows.

energies. Curves (d) show the well known theoretical result that no oscillation is predicted by the free-atom model. The use of form-factor approximations instead of perturbation theory does not change the conclusions: both predict smooth scattering amplitudes in the considered experimental range of x, and consequently, they are unable to explain the experimental peaks due to Bragg scattering.

Figures 2(a) and 3(a) show that, even for $x > 1$ Å^{-1}, diffraction peaks could be detected. Due to TDS, some of them are concealed in the experimental curves (b), more for Pb and less for Pt and W.

In the experiment done with γ rays (c) no peaks are detected at $x > 1$, not only due to TDS but also due to the lower x accuracy when compared to the x-ray experiments.

Comparing curves (a) and (b), one can see, for the Pt and W cases, the effect of preferential grain orientation. In Fig. 2(b) the effect results in a reduction of the (hhh) peaks and an increase of peaks ($h00$). In Fig. 3(b) (W), the preferential grain orientation results in reduction of ($hh0$) peaks and in an increase of ($h00$) peaks, both pointed with arrows.

Comparing curves (b) and (c) one can easily see the effect of different geometrical accuracy. In the X-ray experiment, with a momentum-transfer accuracy 10 times better than the γ one, it is possible to detect peaks on $x = 0.64$ Å^{-1} for Pb and $x = 1.4$ Å^{-1} for Pt and W. In the γ experiment, the largest values of x for which diffraction peaks were detected are $x = 0.5$ Å^{-1} for Pb and $X = 1$ Å^{-1} for Pt and W. Figures 1(c), 2(c), and 3(c) show that, in general, a good agreement between theory and experiment is achieved for $x > 1$ Å^{-1}.

In brief, six parameters are involved in Rayleigh-scattering measurements: chemical element, atomic structure of the sample, temperature, momentum transfer, angular resolution, and the measurement accuracy. For a given sample, for a given temperature, and for a given momentum transfer, the detection of solid-state effects like diffraction peaks depends on the angular resolution and on the measurement accuracy. For the studied elements the momentum-transfer limits for which diffraction peaks are detected lie between 0.5 and 2.0 Å^{-1}.

With respect to the applicability of the free-atom approximation in the analysis of photon elastic scattering, it is convenient to divide momentum transfer into three regions with diffuse limits: small ($x < 1$ Å^{-1}), medium (1 Å$^{-1} < x < 5$ Å^{-1}), and large ($x > 5$ Å^{-1}). For large x, it is well known [3] that the free-atom hypothesis is valid

for any chemical element, independent of the type of sample and temperature. From the present work it is possible to conclude that (1) for medium x, the comparison between experimental data and Rayleigh theories should only be made after testing the occurrence of interference effects; (2) for small x, the solid-state effects cannot be ignored expect in measurements with samples with large B factor, with samples at high temperatures, and in experiments with low accuracy. The limit between the medium and large x ($x=5$ Å^{-1}) should be investigated. Since it is not easy to reach x values larger than 2 with x-ray tubes, synchrotron sources could be used.

ACKNOWLEDGMENTS

We would like to thank Dr. Lynn Kissel for the careful revision of this paper, and the agencies CNPq, FAPERJ, and FINEP for supporting this work.

[1] P. Papatzacos and K. Mork, Phys. Rev. D **12**, 1206 (1975).
[2] O. D. Gonçalves, I. Mazzaro, and C. Cusatis, IRPS-News **4**, 9 (1990).
[3] P. Kanne, L. Kissel, R. Pratt, and P. Roy, Phys. Rep. **140**, 75 (1986).
[4] L. Kissel and R. Pratt, in *Atomic Inner Shell Physics,* edited by B. Crasemann (Plenum, New York, 1985).
[5] R. B. Taylor, P. Teansomprasong, and I. B. Whittingham, Phys. Rev. A **32**, 151 (1985); J. P. Lestone, R. B. Taylor, P. Teansonprasong, and I. B. Whittingham, *ibid.* **37**, 3218 (1988).
[6] J. Eichler, O. D. Gonçalves, and S. de Barros, Phys. Rev. A **37**, 3702 (1988).
[7] D. Schaupp, M. Schumacher, F. Smend, P. Rullhusen, and J. H. Hubbel, J. Phys. Chem. Ref. Data **12**, 467 (1983).
[8] J. H. Hubbel *et al.*, J. Phys. Chem. Ref. Data **4**, 615 (1975).
[9] J. H. Hubbel and I. Overbo, J. Phys. Chem. Ref. Data **8**, 69 (1979).
[10] G. E. Brown, R. E. Peierls, and J. B. Woodward, Proc. R. Soc. London Ser. A **227**, 51 (1955).
[11] O. D. Gonçalves, J. Eichler, and S. de Barros, Nucl. Instrum. Methods **A280**, 375 (1989).
[12] T. Saka and N. Kato, Acta Crystallogr. Sec. A **42**, 469 (1986).
[13] P. J. E. Aldred and M. Hart, Proc. R. Soc. London Ser. A **33**, 223 (1973).
[14] H. A. Graef and J. R. Schneider, Phys. Rev. A **34**, 34 (1986).
[15] C. Cusatis and M. Hart, in *Anomalous Scattering,* edited by Ramaseshan and Abrahams (Munksgaard, Copenhagen, 1975).
[16] B. E. Warren, *X-Ray Diffraction* (Addison-Wesley, Reading, MA, 1969).
[17] *International Tables for X-Ray Crystallography* (Kynoch, Birmingham, 1968).